

# Percutaneous nephrolithotripsy: C-arm CT with 3D virtual navigation in non-dilated renal collecting systems

Dechao Jiao   
 Zhanli Zhang   
 Zhanguo Sun   
 Yanli Wang   
 Xinwei Han 

## PURPOSE

We aimed to evaluate the clinical superiority of using C-arm computed tomography (CT) to establish percutaneous nephrolithotripsy (PCNL) access for patients with non-dilated renal collecting systems.

## METHODS

From May 2014 to May 2015, 33 patients underwent C-arm CT-guided puncture to establish PCNL access after failed attempts of ultrasonography-guided nephrostomy. Technical success, procedure details, radiation exposure, complications, and stone-free rate were recorded.

## RESULTS

The technical success rate was 97% (32/33) with a mean puncture score of 4.5/5. Mean puncture, dilation, and fragmentation times were 17.9±6.0, 12.6±3.9, and 33.1±8.8 minutes, respectively. Mean radiation exposure was 4.8±2.1 mSv without serious complications. Stone-free rate was 93.8%.

## CONCLUSION

C-arm CT is a useful tool to establish PCNL access, particularly in cases of upper pole access or complicated anatomy.

This work was supported by the national high-tech research and development program (863 Program) (grant number: 2015AA020301).

From the Department of Interventional Radiology (D.J., Z.S., Y.W., X.H. ✉ 13592583911@163.com), The First Affiliated Hospital of Zhengzhou University, Zhengzhou, People's Republic of China; Department of Interventional Radiology (Z.Z.), The People's First Hospital of Xinxiang, Henan, People's Republic of China.

ORCID iDs of the authors: D.J. 0000-0002-5055-4672; Z.Z. 0000-0002-9574-7785; Z.S. 0000-0002-3718-0485; Y.W. 0000-0003-4353-7169; X.H. 0000-0002-7938-6617

Received 6 March 2017; revision requested 23 March 2017; last revision received 1 September 2017; accepted 7 September 2017.

Published online 19 December 2017.

DOI 10.5152/dir.2017.17079

The establishment of a percutaneous tract into the renal collecting system is important and requires imaging supervision during percutaneous nephrolithotomy (PCNL) (1, 2). Unlike percutaneous nephrostomy for patients with hydronephrosis, if percutaneous stone removal is planned, the puncture should be performed in a calyx with possible access to the stone. Montvilas et al. (3) demonstrated that ultrasonography (US)-guided techniques yield lower technical success in patients with non-dilated than in those with dilated collecting systems (82% vs. 98.2%). Furthermore, renal anomalies and scoliosis make needle access more challenging and necessitate puncture planning and control. The syngo iGuide navigation system (Siemens Healthcare) is a three-dimensional (3D) virtual needle tracking system which helps predict and observe the needle trajectory, facilitating real-time puncture to the target (4–7). We report our experience of percutaneous tract establishment for patients with non-dilated renal collecting systems after failed US-guided attempts.

## Methods

### Patient selection

This retrospective study was approved by our Institutional Review Board and informed consent was waived. Between May 2014 and May 2015, of 442 patients with non-dilated renal collecting systems who required PCNL access in two urology surgery departments at our hospital, routine US-guided nephrostomy attempts failed in 33 patients (19 males, 14 females; mean age, 60.1±11.8 years) with non-dilated renal collecting systems underwent C-arm computed tomography (CT) with 3D virtual navigation system-guided establishment of PCNL access. A collecting system was identified as non-dilated if no calyceal dilatation was observed on US. All cases had previously failed under US-guidance. The mean body mass index (BMI) was 24.7±4.5 kg/m<sup>2</sup> (range, 17.4–35.9 kg/

You may cite this article as: Jiao D, Zhang Z, Sun Z, Wang Y, Han X. Percutaneous nephrolithotripsy: C-arm CT with 3D virtual navigation in non-dilated renal collecting systems. *Diagn Interv Radiol* 2018; 24: 17–22.

m<sup>2</sup>), and there were 14 (42.4%) overweight patients (defined as BMI >25 kg/m<sup>2</sup> and <40 kg/m<sup>2</sup>). Detailed patient characteristics are listed in Table 1.

### Image acquisition

With patients in the prone position, C-arm CT images were acquired with an Artis zeego flat detector as described by Jiao et al. (7) in a previous study.

### Procedure

Figs. 1–4 demonstrate the various steps of the procedure. After a 3D volume image was reconstructed in the syngo iGuide navigation system, the puncture point at skin and target were selected from multi-planar images. First, the C-arm was rotated to the “bull’s eye view”, then a virtual path was presented and superimposed onto real-time fluoroscopic screen (Fig. 2). The laser positioning system on the flat-panel located the skin entry point (Fig. 2a). After sterile preparation of the area, local anesthesia was administered (5 mL of 1% lidocaine). A 21 G Chiba needle was advanced over the predefined needle path to the correct depth with the needle tip clearly seen touching the renal stone under fluoroscopy during a breath-hold (Fig. 2b–2d). The C-arm was rotated to different angles to monitor the needle progression under real-time fluoroscopy. Another C-arm CT confirmed the correct-needle position (Fig. 3). A contrast agent (Ioversol injection, 300 mgI/mL Hengrui Medical Company) diluted to 30%, was slowly injected to outline the stones, calyx, and pelvis. A 0.018-inch guidewire was inserted into the pelvis-ureter-bladder through the introducer needle, and then a 5 F KMP catheter (Cook Medical) was advanced along the guidewire to establish a safety PCNL access and serve as “security catheter” (Fig. 4a, 4b). Then the patient was transferred to the PCNL operating suite in another building.

### Main points

- C-arm CT, with dual advantages of CT and fluoroscopy, may become the first-choice approach for patients with non-dilated collecting systems.
- C-arm CT is a useful tool to establish percutaneous nephrolithotripsy access, particularly for inexperienced physicians.
- C-arm CT helps avoid surrounding structures to decrease complications.

### PCNL procedures

PCNL procedures were performed under general anesthesia 0.5–3 hours after “security catheter” placement. After positioning a 0.032-inch super stiff wire (Amplatz, Boston Scientific), the security catheter was removed. The tract was dilated with 9 F and 16 F coaxial dilators, and a 16 F peel-away sheath (uroVision GmbH) was passed into the renal pelvis. Stone fragmentation was done with a 8/9.8 F rigid ureteroscope (Richard Wolf); lithotriptors can effectively fragment and aspirate stones easily. After nephroscopy and fluoroscopy were used to assess stone removal, a 16 F nephrostomy catheter was placed for drainage (Fig. 4c).

### Definitions

Technical success was defined as successful placement of the “security catheter”. Puncture score was assessed by three interventional radiologists using a five-point scale (Table 2). Renal access puncture time was defined as the time elapsed from initial C-arm CT scan to security catheter placement. Tract dilation time was defined as time elapsed from insertion of the wire into the security catheter to advancement of the access sheath. Fragmentation time was defined as time elapsed from insertion of the rigid nephroscope to placement of the nephrostomy tube. Complications were categorized by the Clavien-Dindo classification system (8). Patient radiation exposure data

**Table 1.** Patient characteristics

|   |                      |
|---|----------------------|
| Total number of patients  | 33                   |
| Male/female, n  | 19/14                |
| Age (years), mean±SD (range)  | 60.1±11.8 (37–82)    |
| Clinical symptom, n (%)   |                      |
| Hematuria   | 15 (45.5)            |
| Flank and/or abdominal pain   | 6 (18.2)             |
| No symptoms   | 12 (36.3)            |
| Body mass index (kg/m <sup>2</sup> ), mean±SD (range)   | 24.7±4.5 (17.4–35.9) |
| Previous kidney intervention, n   |                      |
| Open surgery  | 3                    |
| PCNL  | 6                    |
| ESWL  | 7                    |
| Stone location/characteristic, n (%)  |                      |
| Calyceal renal stone  | 10 (30.3)            |
| Renal pelvic stone  | 7 (21.2)             |
| Staghorn calculi  | 6 (18.2)             |
| Proximal ureteral stone   | 3 (9.1)              |
| Multiple stones   | 7 (21.2)             |
| Side (left/right), n  | 22/11                |
| Mean stone size (cm), mean±SD (range)   | 3.3±1.5 (1.6–7.0)    |
| ASA physical status, n (%)  |                      |
| Class 1   | 10 (30.3)            |
| Class 2   | 15 (45.5)            |
| Class 3   | 8 (24.2)             |
| Reasons for failed US-guided PCNL, n (%)  |                      |
| Failed guidewire or nephrostomy tube insertions   | 19 (57.6)            |
| Inability to identify calyx   | 8 (24.2)             |
| Anatomic obstacles in potential puncture access   | 6 (18.2)             |
| SD, standard deviation; US, ultrasonography; PCNL, percutaneous nephrolithotripsy; ESWL, extracorporeal shock wave lithotripsy; ASA, American Society of Anesthesiologists. |                      |

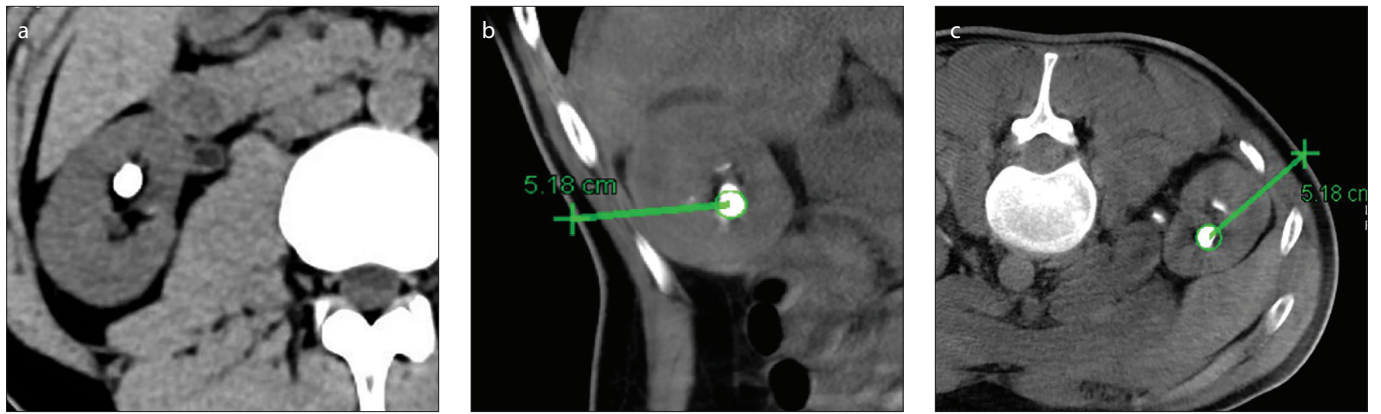


**Figure 1.** a–c. Preoperative CT image (a) shows a renal stone (1.8 cm) in the lower calyx; multiplanar C-arm CT images (b, c) with graphics show the planned needle path (green line) to the target stone (green circle), avoiding damage to the spleen, diaphragm, and lung.

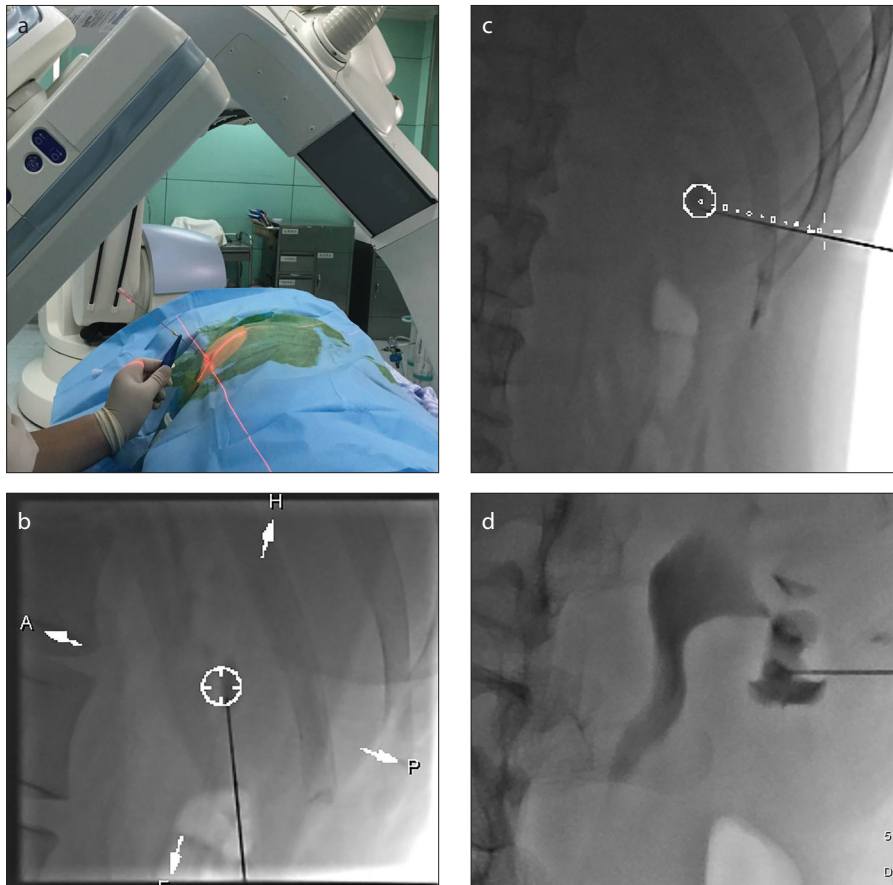


**Figure 2.** a–d. The laser positioning system on the flat-panel locates the skin entry point (a). Real-time fluoroscopic images from bull's eye view (b) and progression view (c): image (c) shows the needle advanced along the planned needle path (dotted line) from the skin entry site (cross) to the target lesion site (circle). Post-contrast injection image (d) clearly shows the stone, renal calyx, and pelvis.

was collected for both C-arm CT and fluoroscopy. Dose area products (DAPs) were converted to effective doses using a conversion factor of  $0.30 \text{ mSv}\cdot\text{Gy}^{-1}\cdot\text{cm}^2$ , which was previously determined by Suzuki et al. (9) who used the same cone-beam CT system.

### Statistical analysis

All data analyses were performed using SPSS software (version 13.0; SPSS Inc.). Quantitative data are presented as mean  $\pm$  standard deviation (SD) and range.

## Results

The technical success rate was 97% (32/33). Puncture locations were in the upper calyx in 18 cases, the middle calyx in 8, and the lower calyx in 6. The mean puncture score was  $4.5 \pm 0.9$ . There were 22 cases (66.7%) punctured on the first pass successfully and given a score of 5. Puncture readjustment was done in 10 cases (30.3%), with 1–2 needle readjustments in six and 3–4 in four. One female patient with severe chronic obstructive pulmonary disease had a 2.5 cm stone in left lower calyx, and puncture readjustments were tried more than 10 times because of her difficulty in holding her breath resulting in low C-arm CT image quality. There was too much contrast around the kidney leading to poor visualization of the collection system and calculus. The case was recorded as a technical failure. The stone-free rate was 93.8%, confirmed by CT scan after the procedures (Fig. 4d). Residual lower calyx stone remained in two patients with giant staghorn calculi due to difficulty reaching them with the nephroscope through a single upper renal calyx access point. Detailed information is listed in Table 3.

One patient (3.1%) experienced fever ( $39.1^\circ\text{C}$ ) one hour after security catheter

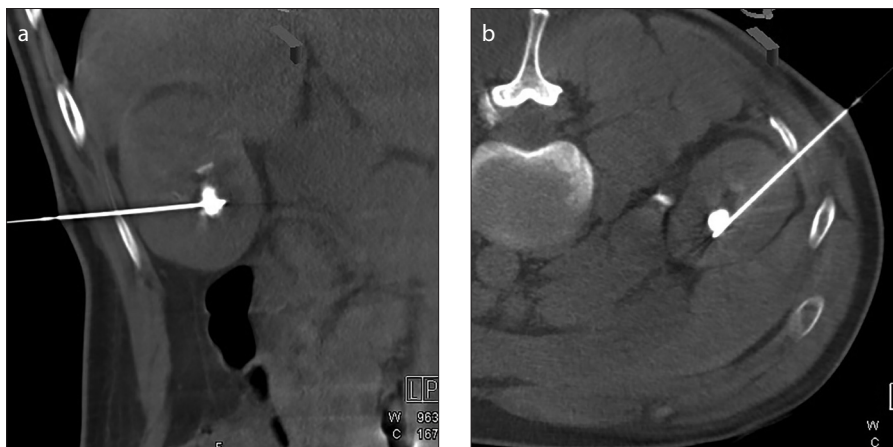
**Table 2.** Scoring standards for evaluation of the puncture performance

| Score | Criteria   |
|-------|--|
| 5     | Successful puncture on first needle pass                                   |
| 4     | Successful puncture required 1–2 needle readjustments                      |
| 3     | Successful puncture required 3–4 needle readjustments                      |
| 2     | Successful puncture required >4 needle readjustments or needle reinsertion |
| 1     | Unsuccessful puncture due to needle positioning error                      |

**Table 3.** Intraoperative and postoperative data

|  |                              |
|--|------------------------------|
| Technical success                        | 32 (97.0)                    |
| Distance from skin to target stone (cm)  | 7.9±1.1 (5.1–11.3)           |
| Puncture performance                     |                              |
| Score 5                                  | 22 (66.7)                    |
| Score 4                                  | 6 (18.2)                     |
| Score 3                                  | 4 (12.1)                     |
| Score 1                                  | 1 (3.0)                      |
| Puncture location                        |                              |
| Upper calyx                              | 18 (56.2)                    |
| Middle calyx                             | 8 (25.0)                     |
| Lower calyx                              | 6 (18.8)                     |
| Mean puncture time (min)                 | 17.9±6.0 (8.5–34.2)          |
| Mean dilation time (min)                 | 12.6±3.9 (6.7–21.0)          |
| Mean fragmentation time (min)            | 33.1±8.8 (15.6–50.1)         |
| Number of C-arm CT acquisitions          | 1.6±0.8 (1–4)                |
| Dose area product (mGy·cm <sup>2</sup> ) | 15 867±7 067 (71 017–36 144) |
| Effective radiation dose (mSV)           | 4.8±2.1 (2.1–10.9)           |
| Mean hospital stay (days)                | 6.4±2.3 (3–15)               |
| Procedure-related complications          |                              |
| Postoperative fever (grade 1)            | 1 (3.0)                      |
| Hemoglobin decline (grade 1)             | 1 (3.0)                      |
| Stone-free status                        |                              |
| Stone-free                               | 30 (93.8)                    |
| Residual stone                           | 2 (6.2)                      |

Data are presented as n (%) or mean±standard deviation (range).

**Figure 3.** a, b. Multiplanar C-arm CT images (a, b) confirm the final position of the needle.

placement, but returned to normal after lysinipirine injection (0.9 g). One elderly patient (3.1%) experienced a decline in hemoglobin (5 g/L) and was given fluid infusion without blood transfusion. These were classified as grade 1 complications.

## Discussion

Establishing renal access has an important impact on the overall outcome of PCNL. US is the used most commonly tool for guidance, with success rates of 88%–99%

and complication rates of 4%–8% (10, 11). US-guidance is effective and radiation-free; it also demonstrates the intrarenal arteries, helping operators avoid vascular injury (12). However, it is technically difficult for inexperienced doctors to establish a renal access for patients without hydronephrosis, due to poor visibility during guidewire manipulation following renal access (13).

Fluoroscopy is another common guidance method; however, it provides no data about surrounding soft tissues. In addition, increased pressure from too much contrast injection may lead to collateral bleeding or sepsis (14). In a prospective randomized trial, Agarwal et al. (15) compared US and US combined with fluoroscopy guidance for PCNL among 224 patients. The mean number of attempts for successful puncture in the desired calyx was 3.3 in group 1 (fluoroscopy guidance) as compared with 1.5 in group 2 (US combined with fluoroscopy guidance). CT provides excellent soft tissue imaging, but it is impractical for intraoperative use because of its environment, large size and location outside the PCNL suite (16). In recent years, C-arm CT with 3D live needle guidance has shown remarkably accurate needle placement during nonvascular interventions (17, 18), and it offers high spatial resolution (<1 mm) and a contrast resolution of 10 HU (adequate amount for very high-density stone and soft tissue).

Our technical success rate was 97% without any severe complications. This favorable outcome suggests that C-arm CT guidance is a reliable tool to establish PCNL access in difficult cases. A total of 22 cases (66.7%) were successfully punctured on the first pass, and all 14 overweight cases were successful in 1–3 attempts in our study. Satisfactory results mean that virtual navigation enabled us to select an accurate and safe needle access to the target stone. The mean procedure time was 63.6 minutes (sum of puncture, dilation and fragmentation time), which is reasonable compared with conventional PCNL procedures (40–180 min) (19, 20). The stone-free rate (93.8%) is similar to that reported in the literature with US guidance (80%–96%) (19, 20), which is reasonable because it only affects the needle pass, and the PCNL is essentially the same as the one performed with US guidance.

In 2012, Roy et al. (21) first reported the use of this novel imaging modality to obtain percutaneous access and evaluate postoperatively for residual fragments, describing it as the best guidance modality. In



**Figure 4. a–d.** C-arm CT image (a) confirms the spatial relationship between the access point and the stone. Image (b) shows a 5 F KMP “security catheter” advanced through the renal pelvis, ureter, and bladder to establish safety PCNL access. Postoperative fluoroscopy (c) and CT (d) show absence of renal calculi after treatment.

2016, Hawkins et al. (22) reported the primary results with C-arm CT needle-guided PCNL in children and adolescents (9 cases), and concluded that it is useful for establishing PCNL access. We believe that C-arm CT guidance has many advantages. First, it allows careful planning of needle insertion such as trajectory, depth, and location before PCNL puncture. Second, the needle tip can precisely puncture the target stone real-time under fluoroscopy. Third, C-arm CT provides detailed soft tissue information to reduce puncture complications. Fourth, it is easy to manipulate the guidewire and catheter following renal access under fluoroscopy. In future, C-arm CT with 3D needle

guidance may become the first-choice approach after US-guidance failure, because it has dual advantages of CT and fluoroscopy.

Complications of percutaneous access (e.g., pleural injury, colon injury, and severe bleeding) can be reduced with better imaging for needle detection and guidance (23). Preoperative bleeding usually results from parenchymal vessels rupture and kidney tear from excessive sheath bending during PCNL access dilation. Traditionally, PCNL access was established within Brodel’s avascular plane through the tip of the calyx, which has been considered as a route that can be easily implemented under C-arm CT guidance without massive bleeding (24). Supra-

costal accesses above eleventh rib should be avoided when other puncture options are available to decrease pneumothorax occurrence (24), which can be easily distinguished by C-arm CT imaging. Employing 3D positioning and real-time virtual navigation in this study, the upper calyx was selected as the puncture target in 18 cases (56.2%) with no complications.

Direct comparisons of radiation DAP values between cone-beam CT systems are usually possible because the systems accurately record radiation results themselves. The effective dose in the study was 4.8 mSv, similar to that in Sailer et al. (25) (4.3 mSv), and lower than the effective dose in abdominal CTs (7 mSv) (26). The mean effective dose has been reported as 6.6 and 13.6 mSv for renal angiography and angioplasty, respectively (27) and as 13.5 mSv for a CT-guided drainage procedure (28). Therefore, C-arm CT radiation dose is not a substantial problem.

Although this method has many advantages, it still has its limitations. Movements and respirations from patients will result in artifacts which may affect puncture accuracy. Furthermore, greater numbers of patients are required, particularly those with BMI >35 kg/m<sup>2</sup>, because evaluation in obese patients is needed to confirm the superiority of C-arm CT over US. Lastly, multifunction digital subtraction angiography was installed in another building in our center. After PCNL safety access establishment, the patient had to be transferred to the PCNL operating suite.

In conclusion, C-arm CT is a useful tool for establishment of PCNL access, avoiding surrounding structures such as bowel, liver and spleen, particularly in cases of upper pole access or complicated anatomy.

#### Conflict of interest disclosure

The authors declared no conflicts of interest.

#### References

- Ozgor F, Ucpinar B, Binbay M. Effect of obesity on prone percutaneous nephrolithotomy outcomes: a systemic review. *Urol J* 2016; 13:2471–2478.
- Pradeepa MG, Sinha MM, Tyagi K. The halo sign during a percutaneous nephrolithotomy puncture. *Can Urol Assoc J* 2016; 10:E130. [CrossRef]
- Montvilas P, Solvig J, Johansen TE. Single-centre review of radiologically guided percutaneous nephrostomy using “mixed” technique: success and complication rates. *Eur J Radiol* 2011; 80:553–558. [CrossRef]
- Jiao D, Yuan H, Zhang Q, et al. Flat detector C-arm CT-guided transthoracic needle biopsy of small ( $\leq 20$  cm) pulmonary nodules: diagnostic accuracy and complication in 100 patients. *Radiol Med* 2016; 121:268–278. [CrossRef]

5. Jiao D, Xie N, Wu G, et al. C-arm cone-beam computed tomography with stereotactic needle guidance for percutaneous adrenal biopsy: initial experience. *Acta Radiol* 2017; 58:617–624. [\[CrossRef\]](#)
6. Kim TH, Park CM, Lee SM, et al. Percutaneous transthoracic localization of pulmonary nodules under C-arm cone-beam CT virtual navigation guidance. *Diagn Interv Radiol* 2016; 22:224–230. [\[CrossRef\]](#)
7. Jiao de C, Li TF, Han XW, et al. Clinical applications of the C-arm cone-beam CT-based 3D needle guidance system in performing percutaneous transthoracic needle biopsy of pulmonary lesions. *Diagn Interv Radiol* 2014; 20:470–474. [\[CrossRef\]](#)
8. de la Rosette JJ, Opondo D, Daels FP, et al. Categorisation of complications and validation of the Clavien score for percutaneous nephrolithotomy. *Eur Urol* 2012; 62:246–255. [\[CrossRef\]](#)
9. Suzuki S, Furui S, Yamaguchi I, et al. Effective dose during abdominal three-dimensional imaging with a flat-panel detector angiography system. *Radiology* 2009; 250:545–550. [\[CrossRef\]](#)
10. Chen ML, Shukla G, Jackman SV, et al. Real-time tomographic reflection in facilitating percutaneous access to the renal collecting system. *J Endourol* 2011; 25:743–745. [\[CrossRef\]](#)
11. Radecka E, Brehmer M, Holmgren K, et al. Complications associated with percutaneous nephrolithotripsy: supra- versus subcostal access. A retrospective study. *Acta Radiol* 2003; 44:447–451. [\[CrossRef\]](#)
12. Song Y, Ma Y, Song Y, et al. Evaluating the learning curve for percutaneous nephrolithotomy under total ultrasound guidance. *PLoS One* 2015; 10:e0132986. [\[CrossRef\]](#)
13. Usawachintachit M, Masic S, Chang HC, et al. Ultrasound guidance to assist percutaneous nephrolithotomy reduces radiation exposure in obese patients. *Urology* 2016; 98:32–38. [\[CrossRef\]](#)
14. Jagtap J, Mishra S, Bhattu A, et al. Which is the preferred modality of renal access for a trainee urologist: ultrasonography or fluoroscopy? Results of a prospective randomized trial. *J Endourol* 2014; 28:1464–1469. [\[CrossRef\]](#)
15. Agarwal M, Agrawal MS, Jaiswal A, et al. Safety and efficacy of ultrasonography as an adjunct to fluoroscopy for renal access in percutaneous nephrolithotomy (PCNL). *BJU Int* 2011; 108:1346–1349. [\[CrossRef\]](#)
16. Chi Q, Wang Y, Lu J, et al. Ultrasonography combined with fluoroscopy for percutaneous nephrolithotomy: an analysis based on seven years single center experiences. *Urol J* 2014; 11:1216–1212.
17. Sang ML, Chang MP, Kyung HL, et al. C-arm cone-beam CT-guided percutaneous transthoracic needle biopsy of lung nodules: clinical experience in 1108 patients. *Radiology* 2013; 271:291–300.
18. Jin KN, Park CM, Goo JM, et al. Initial experience of percutaneous transthoracic needle biopsy of lung nodules using C-arm cone-beam CT systems. *Eur Radiol* 2010; 20:2108–2115. [\[CrossRef\]](#)
19. Knoll T, Daels F, Desai J, et al. Percutaneous nephrolithotomy: technique. *World J Urol* 2017; 35:1361–1368. [\[CrossRef\]](#)
20. Wang J, Yang Y, Chen M, et al. Laparoscopic pyelolithotomy versus percutaneous nephrolithotomy for treatment of large renal pelvic calculi (diameter >2 cm): a meta-analysis. *Acta Chir Belg* 2016; 116:346–356. [\[CrossRef\]](#)
21. Roy OP, Angle JF, Jenkins AD, et al. Cone beam computed tomography for percutaneous nephrolithotomy: initial evaluation of a new technology. *J Endourol* 2012; 26:814–818. [\[CrossRef\]](#)
22. Hawkins CM, Kukreja K, Singewald T, et al. Use of cone-beam CT and live 3-D needle guidance to facilitate percutaneous nephrostomy and nephrolithotripsy access in children and adolescents. *Pediatr Radiol* 2016; 46:570–574. [\[CrossRef\]](#)
23. Rais-Bahrami S, Friedlander JJ, Duty BD, et al. Difficulties with access in percutaneous renal surgery. *Ther Adv Urol* 2011; 3:59–68. [\[CrossRef\]](#)
24. Kyriazis I, Panagopoulos V, Kallidonis P, et al. Complications in percutaneous nephrolithotomy. *World J Urol* 2015; 33:1069–1077. [\[CrossRef\]](#)
25. Sailer AM, Schurink G, Wildberger J, et al. Radiation exposure of abdominal cone beam computed tomography. *Cardiovasc Intervent Radiol* 2015; 38:112–120. [\[CrossRef\]](#)
26. Braak SJ, van Strijen MJ, van Es HW, et al. Effective dose during needle interventions: cone-beam CT guidance compared with conventional CT guidance. *J Vasc Interv Radiol* 2011; 22: 455–461. [\[CrossRef\]](#)
27. Ruiz Cruces R, García-Granados J, Diaz Romero FJ, et al. Estimation of effective dose in some digital angiographic and interventional procedures. *Br J Radiol* 1998; 71:42–47. [\[CrossRef\]](#)
28. Teeuwisse WM, Geleijns J, Broerse JJ, et al. Patients and staff dose during CT guided biopsy, drainage and coagulation. *Br J Radiol* 2001; 74:720–726. [\[CrossRef\]](#)